Maritime Technology and Engineering 3 – Guedes Soares & Santos (Eds)

Assessment of the performance and the exhaust emissions of a marine diesel engine for different start angles of combustion

M. Tadros, M. Ventura & C. Guedes Soares
Centre for Marine Technology and Ocean Engineering (CENTEC), Instituto Superior Técnico, Universidade de Lisboa, Lisbon, Portugal

ABSTRACT: The start angle of combustion plays an important role in determining the performance and the exhaust emissions of a diesel engine. In this paper, the assessment of the behavior of a marine diesel engine is presented for twelve start angles of combustion. The simulation is done using a 1D engine simulation code developed and implemented in Matlab, which was validated with a commercial software tool. Three engine speeds are considered during the simulation. The optimum range of crank angles to start the combustion is determined for engine optimization. The heat release rate and the Wiebe function are used to determine the behavior of the combustion process. The amount of carbon dioxide (CO_2) and nitrogen oxide (NO_x) emissions are calculated for the different cases assumed. The simulation results are compared with data taken from a real engine.

1 INTRODUCTION

Due to the new regulations adopted by the international maritime organization (IMO) (http://www.imo.org), the behavior of the marine diesel engines must be adjusted to fit these restricted regulations for the different speeds of the engine.

The combustion process in compression ignition (CI) diesel engines plays an effective role to control both the performance and the exhaust emissions.

In a diesel engine, the ignition occurs when mixture of fuel and air is exposed to the appropriate conditions of temperature and equivalence ratio. The auto-ignition temperature is considered the temperature at which a substance can be brought to flames without any sort of external force, such as a flame or spark. It varies from 450 to 602 K according to the type of fuel used.

The compression ratio of the engine is increased along the different levels (tiers) applied by the IMO. In tier 1 engines, the compression ratio varies from 11 to 12, this value is then increased from 14 to 15 in tier 2 and can reach 17 in tier 3 (http://marine.man.eu/). A high compression ratio is desirable because it allows the engine to extract more mechanical energy from a given mass of air-fuel mixture due to its higher thermal efficiency by increasing the burn rate of the injected fuel inside the cylinder.

The adjustment of the auto-ignition point, to determine the combustion process of a diesel engine, is difficult due to the variations of the amount and the properties of the fuel used and the compressed air. The injection timing and the ignition delay are two common points that must be considered to compute the exact ignition timing Hardenberg and Hase (1979) present an empirical formula in terms of pressure, temperature, mean piston speed and cetane number (CN) of the fuel used to predict the ignition delay in direct injection (DI) engines. This formula is used by Watson et al. (1980) to determine the Wiebe function of CI diesel engines to present the amount of the burned mass fraction in the premixed, diffusion and tail stages. By calculating the delay in the auto-ignition point, the behavior of the combustion process using the net heat release rate (HRR) is determined according to the pressure, temperature and volume of the cylinder as presented in (Heywood, 1988) using the first law of thermodynamics.

The study of the injection timing to optimize the engine performance has been done in previous research. Amba Prasad Rao & Kaleemuddin (2011) present an experimental study on a 510 cc automotive type naturally aspirated, water-cooled, direct injection diesel engine operated with variable timing fuel injection cam and show a significant reductions in NO_x and smoke emission levels, each one separately using the higher fuel-line and the high combustion pressures for better combustion by adopting the injection timing. Kalghatgi et al. (2011) run a single-cylinder diesel engine on gasolines of different octane numbers at different operating conditions. The auto-ignition quality of the fuel is described by an Octane Index. It has been shown that the premixed combustion in the diesel engine is facilitated with higher ignition delays. Also, if two fuels have similar combustion phasing at the same injection timing, their emissions is also similar.

The influence of injection timing on the engine performance and the exhaust emissions is studied by Rahman et al. (2014), using different alternative fuels as diesel, biodiesel, alcohol. In the case of diesel fuel, the advancement in injection timing results in lower carbon monoxide (CO) and hydrocarbon (HC) emissions and increases the NO_x emission. Also, the brake thermal efficiency (BTE) increases and there is a reduction in the brake specific fuel consumption (BSFC). Biodiesel–diesel blends produce more HC and CO emissions with a reduction in NO_x emissions when the injection timing is retarded. However, Agarwal et al. (2013) consider the effect of different fuel injection pressure (FIP) and injection timings on the performance, emissions and combustion of a diesel engine. The advanced injection timings show a rapid combustion. The engine performance is increased at low FIPs accompanied with a lower mass emission of CO_2, CO, HC and NO_x. Zhang et al. (2015), Imtenan et al. (2015) and Wamankar & Murugan (2015) support the same concept of injection timing and pressure on the engine performance that when the combustion process takes place earlier, leads to a reduction in SFC and exhaust gas temperature.

Computational fluid dynamics (CFD) code is used by Raeie et al. (2014) with an improved spray model to simulate the combustion process of diesel with different injection timings and different injection pressures and shows a lower soot and higher NO_x emissions formation in the early injection than the later one.

The effect of the exhaust gas recirculation (EGR) and Miller cycle is added in (Verschaeren et al., 2014) on the injection timing. The use of a high-pressure cooled EGR loop shows a significant decrease in NO_x emissions with increasing EGR% up to 70% at different loads which make the engine work under Tier 3. Saravanan (2015) show by experiment an increase in heat release rate and combustion duration when combining between the advanced injection timing and EGR.

Different types of fuel are used to estimate the engine performance and emissions. The Annona methyl ester (A20) is used in comparing with diesel fuel in (Senthil et al., 2015) for different injecting timing and compression ignition. It shows an increase in brake thermal efficiency and HRR accompanied with a reduction in HC, CO and NO_x emissions. Also, the A20 will be more economical than the diesel fuel. However, Yadav et al. (2015) shows a reduction in emissions when retarded the injection timing and increase in engine power when using WTO (waste transformer oil) in diesel engine.

In the present work, the behavior of the engine cycle is calculated according to different start angles of combustion (SAC) related to the top dead center (TDC) ignoring the timing and the pressure of the injected fuel. Twelve angles are considered, varying from 25 degree BTDC to 25 degree ATDC. The Wiebe function and the heat release rate are used to compute the amount of pressure and temperature rise during the combustion.

3.3 show the schematic diagram of the simulation model. The different components and processes of the engine and the attached turbocharger are presented in details in (Tadros et al., 2015).

Ricardo WAVE (Ricardo Wave Software, 2014) and a code implemented in Matlab are used and the output results are compared and validated using a real marine diesel engine. The performances of the engine expressed in brake power and specific fuel consumptions are calculated for three different engine speeds for the different SAC. The rate of NO_x and CO_2 emissions are calculated for the different cases. These specific emissions are taking into consideration due to their relations with the IMO regulations, the NO_x with the Tiers limits and the CO_2 for the energy efficiency design index (EEDI). An optimum range of the start angles of combustion is determined for each engine speed in accordance to both the engine performance and the exhaust emissions.

2 GOVERNING EQUATIONS

2.1 *Wiebe function and heat release rate*

The Wiebe function is used to estimate the mass fraction burned as a function of engine position and expressed as (Watson et al., 1980):

$$\begin{aligned} x_b &= p_f \left\{1-\left[1-(0.75\tau)^2\right]^{5000}\right\} \\ &+d_f \left\{1-\left[1-(cd_3\tau)^{1.75}\right]^{5000}\right\} \\ &+t_f \left\{1-\left[1-(ct_3\tau)^{2.5}\right]^{5000}\right\} \end{aligned} \quad (1)$$

where x_b is the mass fraction burned, p_f, d_f, t_f, are the mass fractions of the premix, diffusion, and tail burn curves, respectively. cd_3, ct_3, are the burn duration coefficients for the diffusion and tail burn curves, respectively and τ is the burn duration in degrees calculated according to the following expression:

$$\tau = \frac{\theta-\theta_o}{125\left(\frac{RPM}{BRPM}\right)^{0.3}} \quad (2)$$

where θ is the crank angle, θ_o is crank angle at start of combustion, RPM is the engine speed and $BRPM$ is the reference engine speed.

2.2 *The first law of thermodynamics*

The change in pressure, $dP/d\theta$, and change in temperature, $dT/d\theta$, along the crank angle are calculated using the first law of thermodynamics as in the following equations (Heywood, 1988):

$$\frac{dP}{d\theta} = \frac{K-1}{V}\frac{dQ}{d\theta} - \frac{KP}{V}\frac{dV}{d\theta} \quad (3)$$

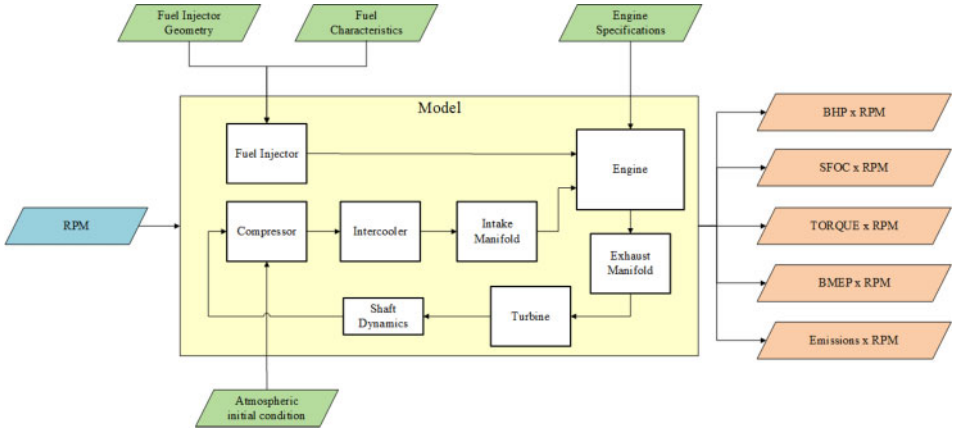

Figure 1. Schematic diagram of the simulation model.

$$\frac{dT}{d\theta} = (K-1)\frac{T}{PV}\left[\frac{dQ}{d\theta} - P\frac{dV}{d\theta}\right] \quad (4)$$

where K is heat specific ratio, V, P, T are the cylinder volume, pressure and temperature respectively, $dV/d\theta$ is the change in volume and dQ is the total heat added.

The total heat added, dQ, takes into account the heat release rate during the combustion, Q_{comb}, and the heat exchanged, dQ_w, with the cylinder walls as presented in (Woschni, 1967):

$$dQ = Q_{comb}dx_b - dQ_w \quad (5)$$

$$Q_{comb} = m_{fuel}CV \quad (6)$$

$$dQ_w = \frac{hA_w}{\omega}(T_g - T_w)d\theta \quad (7)$$

$$h = 3.26B^{-0.2}p^{0.8}T^{-0.55}w^{0.8} \quad (8)$$

where h is the heat transfer coefficient suggested by Woschni, A_w is the area of cylinder walls, ω is the engine speed, T_g is the burn gas temperature, T_w is the cylinder wall temperature, B is the cylinder wall, p is the cylinder pressure and w is the average cylinder gas velocity.

3 GENERAL PRESENTATION OF THE ENGINE

The engine chosen to validate the model is the MAN R6-730 marine engine, a 4-stroke, 6 cylinder in-line, with a speed range of 1,000-2,100 RPM (http://www.engines.man.eu/). It is designed for the propulsion of small boats like yachts and patrol boats.

The maximum power of the MAN R6-730 is 537 kW at 2,300 RPM and the following table shows the main characteristics of the engine. The intake pressure and temperature are set at atmospheric conditions, i.e. 100 KPa and 298 K, respectively. The cylinder wall and piston temperatures are assumed to remain constant along the engine cycle at 500 and 525 K, respectively. The maximum power is 537 kW at 2300 RPM and the following table shows the main information of the engine.

Table 1. Technical data of MAN R6-730.

Bore (mm)	128
Stroke (mm)	166
No. of cylinders	6
Displacement (liter)	12.82
BMEP (bar)	21.9
Piston speed (m/s)	10.5
Engine speed range (RPM)	1,000-2,100
Specific fuel consumption (g/kW.h)	225
Power-to-weight ratio (kW/kg)	0.41

4 RESULTS AND VALIDATION

The simulation results are calculated using a code developed using Matlab which is compared with the results of Ricardo WAVE. The numerical tests are done for three different engine speeds (1,000 – 1,800 – 2,300 RPM) and for twelve start angles for combustion vary from 25 BTDC to 25 ATDC according to the input data presented in 3.3. The reinitialization of model between the different cases is considered during simulation where each case is started with its initial conditions. The purpose of these simulations is to optimize the behavior of a marine diesel engine taking into consideration both the performance and the exhaust emissions.

Figure 2 shows a good fitting between the values of the brake power calculated by the simulation codes. However in Figure 3, the SFC presented is from Matlab calculation only for better overview and correspond to each brake power presented in Figure 2, where it is minimized at the maximum brake power and vice-versa. According to these results, the pressure and

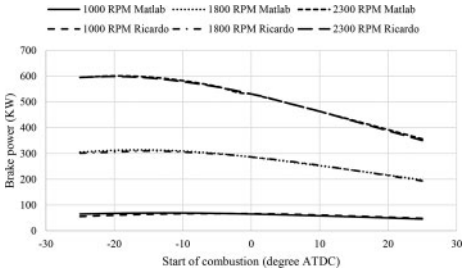

Figure 2. A comparison between the engine brake powers calculated from Matlab code and Ricardo WAVE.

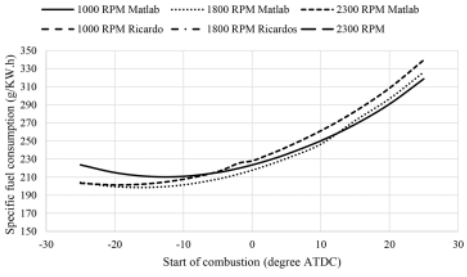

Figure 3. The SFC calculated from Matlab code.

temperature diagram inside the cylinder are calculated and presented in figures 4 to 6.

From the three pressure diagrams in figures 7 to 12 and the brake power shown in Figure 2, the work done by the cylinder is the maximum at the earliest SAC (25 degree BTDC) with values up to 12% greater than the reference value (537 kW) and shows a reduction of up to 45% when the SAC is retarded to 25 degree ATDC. Also, the three temperature diagrams show the greatest rise in temperature in the earliest combustion that pass the 2,000 K and show a reduction in the cylinder temperature with the retardation of the angles of combustion.

The CO_2 and NO_x emissions are calculated from the equilibrium of the equation of combustion and presented in figures Figure 2 to **12**. The rate of CO_2 emissions presented in g/kW.h shows its lowest value between the SAC from -10 to -5 degree ATDC for 1,000 RPM. However, at 1,800 and 2,500 RPM, the minimum value varies between -25 to -5 degrees ATDC. The NO_x emissions presented in the same units as CO_2 emissions show the lowest value from -25 to -5 ATDC at the three different speeds. However, the NO_x emissions in ppm (parts per million) depend on the maximum temperature of combustion and show its lowest values after the TDC.

The percentage change of the values of the calculated results is presented in 5 for the different start angles of combustion in relation with the current one used. The brake power, brake mean effective pressure and engine torque show the same values of variation for the different speeds. They show an increase up to 12% and a reduction up to 35% from the original

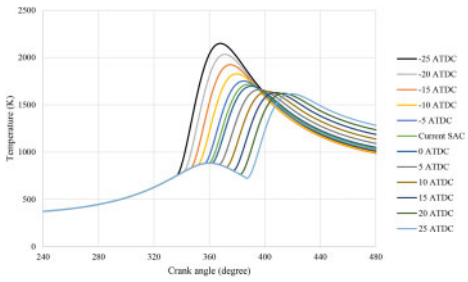

Figure 4. Temperature diagram for different SAC at 1,000 RPM.

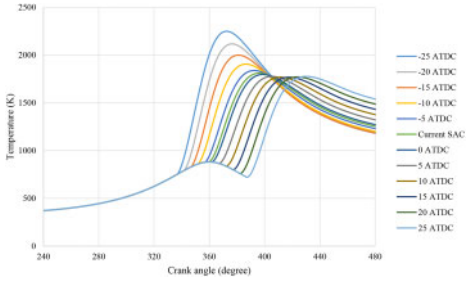

Figure 5. Temperature diagram for different SAC at 1,800 RPM.

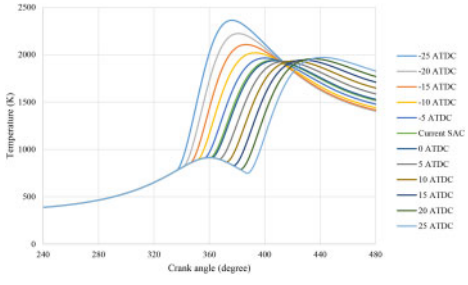

Figure 6. Temperature diagram for different SAC at 2,300 RPM.

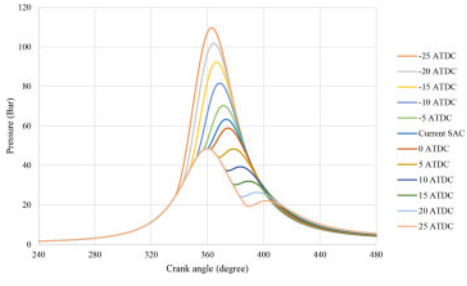

Figure 7. Pressure diagram for different SAC at 1,000 RPM.

value. However, the specific fuel consumption shows a reduction up to 11% and an increase up to 55%.

The maximum temperature of combustion shows a 25% increase than the original value in the earlier combustion, which increase the NO_x emissions by 189%.

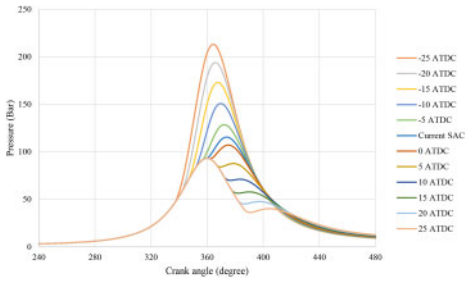

Figure 8. Pressure diagram for different SAC at 1,800 RPM.

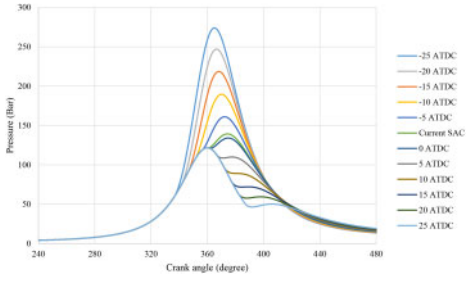

Figure 9. Pressure diagram for different SAC at 2,300 RPM.

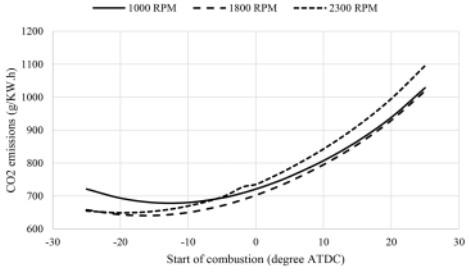

Figure 10. CO_2 emissions calculated for different SACs and different speeds.

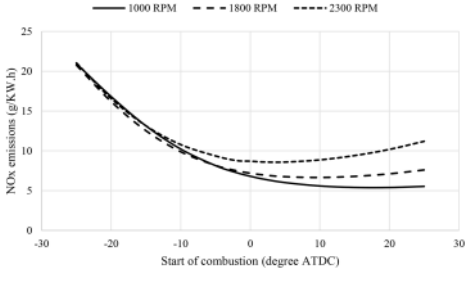

Figure 11. NO_x emissions calculated for different SACs and different speeds.

However, the CO_2 emissions show a 53% increases when the combustion is retarded.

From all the previous figures presented, it is recommended to use variable injection timing for the different engine speed to adjust the SAC to vary from -10 to 10 degree ATDC to reach the lowest level of

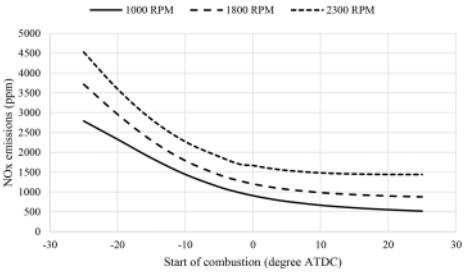

Figure 12. NOx emissions in ppm calculated for different SACs and different speeds.

emissions in relation with the engine performance. From -5 ATDC to 10 degree ATDC, the lowest engine speed reaches its lowest level of NO_x emissions with a little reduction in the brake power and an increase in CO_2 emissions. However, the NO_x emissions is the minimum in the range before the TDC by 10 degree with a suitable engine brake power which increase with the earlier SAC and an acceptable range of CO_2 emissions that decrease with the earliest SAC.

The maximum temperature of combustion shows a 25% increase than the original value in the earlier combustion, which increase the NO_x emissions by 189%. However, the CO_2 emissions show a 53% increases when the combustion is retarded.

From all the previous figures presented, it is recommended to use variable injection timing for the different engine speed to adjust the SAC to vary from -10 to 10 degree ATDC to reach the lowest level of emissions in relation with the engine performance. From -5 ATDC to 10 degree ATDC, the lowest engine speed reaches its lowest level of NO_x emissions with a little reduction in the brake power and an increase in CO_2 emissions. However, the NO_x emissions is the minimum in the range before the TDC by 10 degree with a suitable engine brake power which increase with the earlier SAC and an acceptable range of CO_2 emissions that decrease with the earliest SAC.

5 CONCLUSIONS

This paper shows the effect of the start angle of combustion (SAC) on the performance of the engine and the exhaust emissions for different engine speeds. The results are computed for different SAC values, before, after and at the top dead center (TDC) of the cylinder. The simulation is done using a code developed using Matlab and is compared with the results of Ricardo WAVE for the purpose of validation. The pressure and temperature along the cycle is calculated as a function of the crank angle. The Wiebe function and the net heat release rate are used to determine the behavior of the combustion process. The engine brake power, specific fuel consumption, brake mean effective pressure, engine torque and exhaust emissions are the main output results.

Table 2. Change in percentage of the value of different items for the different SAC related to the original case.

Items	Engine Speed	Start angle of combustion (ATDC) −25	−20	−15	−10	−5	0	5	10	15	20	25
Brake power	1000	–1.73	2.19	4.27	4.22	2.12	–1.69	–6.62	–12.18	–18.15	–24.45	–31.07
	1800	4.57	6.92	7.39	5.91	2.66	–1.99	–7.49	–13.43	–21.71	–28.09	–34.59
	2300	10.85	11.91	11.12	8.51	4.28	–1.16	–7.31	–13.76	–20.33	–26.97	–33.67
Specific fuel consumption	1000	1.76	–2.15	–4.10	–4.05	–2.08	1.72	7.09	13.87	22.17	32.37	45.07
	1800	–4.37	–6.47	–6.89	–5.58	–2.59	2.03	8.10	15.51	27.73	39.07	52.89
	2300	–9.79	–10.64	–10.01	–7.84	–4.11	1.17	7.89	15.96	25.52	36.94	50.76
Brake mean effective pressure	1000	–1.73	2.19	4.27	4.22	2.12	–1.69	–6.62	–12.18	–18.15	–24.45	–31.07
	1800	4.57	6.92	7.39	5.91	2.66	–1.99	–7.49	–13.43	–21.71	–28.09	–34.59
	2300	10.85	11.91	11.12	8.51	4.28	–1.16	–7.31	–13.76	–20.33	–26.97	–33.67
Torque	1000	–1.73	2.19	4.27	4.22	2.12	–1.69	–6.62	–12.18	–18.15	–24.45	–31.07
	1800	4.57	6.92	7.39	5.91	2.66	–1.99	–7.49	–13.43	–21.71	–28.09	–34.59
	2300	10.85	11.91	11.12	8.51	4.28	–1.16	–7.31	–13.76	–20.33	–26.97	–33.67
CO2 emissions	1000	1.73	–2.16	–4.10	–4.05	–2.08	1.72	7.09	13.87	22.17	32.37	45.07
	1800	–4.42	–6.49	–6.89	–5.59	–2.59	2.03	8.10	15.51	24.37	35.02	47.99
	2300	–9.90	–10.69	–10.03	–7.85	–4.11	1.17	7.89	15.96	25.52	36.93	50.76
NOx emissions	1000	188.53	131.50	80.88	40.75	12.14	–6.33	–17.26	–23.14	–25.68	–25.80	–23.87
	1800	176.66	115.59	66.92	31.70	8.80	–4.20	–10.13	–11.39	–9.54	–5.30	1.22
	2300	139.74	88.67	49.72	22.82	6.63	–0.93	–2.17	0.93	7.13	15.96	27.56

**Positive sign denotes the increase in percentage and vice versa.

It has been shown that the variable injection timing can be used to control the angle of the start of combustion for engine optimization, taking into consideration both the engine performance and the exhaust emissions. The SAC at lowest speed of the engine is retarded ATDC, which shows a reduction in the exhaust emissions accompanied with a little decrease in the brake power. However, for the high speeds of the engine, it is required to start the combustion before the TDC to minimize the formation of the exhaust emissions with little change in the value of the brake power.

ACKNOWLEDGEMENTS

This work was performed within the project SHOPERA - Energy Efficient Safe SHip OPERAtion, which was partially funded by the EU under contract 605221.

REFERENCES

Agarwal, A. K., Srivastava, D. K., Dhar, A., Maurya, R. K., Shukla, P. C. & Singh, A. P. 2013. Effect of fuel injection timing and pressure on combustion, emissions and performance characteristics of a single cylinder diesel engine. *Fuel*, 111, 374–383.

Amba Prasad Rao, G. & Kaleemuddin, S. 2011. Development of variable timing fuel injection cam for effective abatement of diesel engine emissions. *Applied Energy*, 88, 2653–2662.

Hardenberg, H. O. & Hase, F. W. 1979. An empirical formula for computing the pressure rise delay of a fuel from its cetane number and from the relevant parameters of direct-injection diesel engines. SAE paper 790493, SAE Trans, vol. 88.

Heywood, J. B. 1988. *Internal combustion engine fundamentals*, McGraw-Hill.

Imtenan, S., Ashrafur Rahman, S. M., Masjuki, H. H., Varman, M. & Kalam, M. A. 2015. Effect of dynamic injection pressure on performance, emission and combustion characteristics of a compression ignition engine. *Renewable and Sustainable Energy Reviews*, 52, 1205–1211.

Kalghatgi, G. T., Hildingsson, L., Harrison, A. J. & Johansson, B. 2011. Autoignition quality of gasoline fuels in partially premixed combustion in diesel engines. *Proceedings of the Combustion Institute*, 33, 3015–3021.

Raeie, N., Emami, S. & Karimi Sadaghiyani, O. 2014. Effects of injection timing, before and after top dead center on the propulsion and power in a diesel engine. *Propulsion and Power Research*, 3, 59–67.

Rahman, S. M. A., Masjuki, H. H., Kalam, M. A., Sanjid, A. & Abedin, M. J. 2014. Assessment of emission and performance of compression ignition engine with varying injection timing. *Renewable and Sustainable Energy Reviews*, 35, 221–230.

Ricardo Wave Software 2014. WAVE 2014.2 Help System.

Saravanan, S. 2015. Effect of EGR at advanced injection timing on combustion characteristics of diesel engine. *Alexandria Engineering Journal*, 54, 339–342.

Senthil, R., Silambarasan, R. & Ravichandiran, N. 2015. Influence of injection timing and compression ratio on performance, emission and combustion characteristics of Annona methyl ester operated diesel engine. *Alexandria Engineering Journal*, 54, 295–302.

Tadros, M., Ventura, M. & Guedes Soares, C. 2015. Numerical simulation of a two-stroke marine diesel engine. *In:* Guedes Soares, C., Dejhala, R., Pavletic, D. (eds.) *Towards Green Marine Technology and Transport.* Taylor & Francis Group, pp. 609–618.

Verschaeren, R., Schaepdryver, W., Serruys, T., Bastiaen, M., Vervaeke, L. & Verhelst, S. 2014. Experimental study of NOx reduction on a medium speed heavy duty diesel engine by the application of EGR (exhaust gas recirculation) and Miller timing. *Energy*, 76, 614–621.

Wamankar, A. K. & Murugan, S. 2015. Effect of injection timing on a DI diesel engine fuelled with a synthetic fuel blend. *Journal of the Energy Institute*, 88, 406–413.

Watson, N., Pilley, A. D. & Marzouk, M. 1980. A Combustion Correlation for Diesel Engine Simulation. SAE Paper 800029.

Woschni, G. 1967. A Universally Applicable Equation for the Instantaneous Heat Transfer Coefficient in the Internal Combustion Engine. SAE Technical Paper 670931.

Yadav, S. P. R., Saravanan, C. G. & Kannan, M. 2015. Influence of injection timing on DI diesel engine characteristics fueled with waste transformer oil. *Alexandria Engineering Journal*, 54, 881–888.

Zhang, Q., Li, M. & Shao, S. 2015. Combustion process and emissions of a heavy-duty engine fueled with directly injected natural gas and pilot diesel. *Applied Energy*, 157, 217–228.